

# Determining matrix elements and resonance widths from finite volume: the dangerous $\mu$ -terms

G. Takács

HAS Theoretical Physics Research Group  
1117 Budapest, Pázmány Péter sétány 1/A, Hungary

9th October 2011

## Abstract

The standard numerical approach to determining matrix elements of local operators and width of resonances uses the finite volume dependence of energy levels and matrix elements. Finite size corrections that decay exponentially in the volume are usually neglected or taken into account using perturbation expansion in effective field theory. Using two-dimensional sine-Gordon field theory as “toy model” it is shown that some exponential finite size effects could be much larger than previously thought, potentially spoiling the determination of matrix elements in frameworks such as lattice QCD. The particular class of finite size corrections considered here are  $\mu$ -terms arising from bound state poles in the scattering amplitudes. In sine-Gordon model, these can be explicitly evaluated and shown to explain the observed discrepancies to high precision. It is argued that the effects observed are not special to the two-dimensional setting, but rather depend on general field theoretic features that are common with models relevant for particle physics. It is important to understand these finite size corrections as they present a potentially dangerous source of systematic errors for the determination of matrix elements and resonance widths.

## 1 Introduction

The matrix elements of local operators (form factors) are central objects in quantum field theory. Indeed they are the subject of considerable interest in lattice QCD, where – among other applications – they are relevant in describing the weak decays of hadrons. Due to the Maiani-Testa no-go theorem [1], it is necessary to extract them using finite-size methods, which are the subject of a seminal paper by Lellouch and Lüscher [2] (see also [3]). A closely related problem is description of resonances, whose decay width can also be extracted from finite-size data, for which the first proposal was made by Lüscher [4].

Two-dimensional integrable quantum field theories provide an ideal testing ground for these ideas because in many such models the exact analytic expressions of the form factors are known. First, the  $S$  matrix can be obtained exactly in the framework of factorized scattering developed in [5] (for a later review see [6]). It was shown in [7] that it is possible to obtain a set of equations satisfied by the form factors using the exactly known scattering amplitudes as input. The complete system of form factor equations, which provides the

basis for a programmatic approach (the so-called form factor bootstrap) was proposed in [8]. For a detailed and thorough exposition of the subject we refer to [9].

On the other hand, for two-dimensional theories there is a very efficient alternative to lattice field theory to evaluate finite size spectra and matrix elements called the truncated conformal space approach, which was first proposed by Yurov and Zamolodchikov [10].

Recently we used this framework to perform a detailed analysis of resonances and local operator matrix elements. Resonances were studied in [11], where it was argued that they can be extracted with a much better accuracy from level splittings than from the slope method originally proposed in [4]. It was realized that the proposed method (dubbed the “improved mini-Hamiltonian” method) is essentially equivalent to determining the matrix element of the interaction term responsible for the decay, and in [12, 13] we explored an approach to treat general matrix elements of local operators, which is an extension of the Lellouch-Lüscher approach. A proof given in [12] shows that results obtained in this framework are valid to all orders in the inverse volume  $1/L$ , i.e. up to corrections decaying exponentially with the volume. We also realized that these so-called “residual” finite size corrections could play an important role, but the tools to study a particular class of these, the so-called  $\mu$ -terms were only developed later by Pozsgay in [14].

In this work the issue of  $\mu$ -terms is addressed in more details. The testing ground is a specific version of the well-known sine-Gordon theory, the so-called  $k$ -folded model [15], mainly because all the necessary techniques are well-developed and the model is thoroughly understood from the theoretical point of view. This work can also be considered as a refinement of the form factor study performed in [16], where the relevance of  $\mu$ -terms was pointed out, but their detailed analysis was omitted.

The main goal of this paper is to present the issues in a way that leads to conclusions which are expected to be relevant to a wide class of models, and in particular to the ongoing efforts to determine resonance parameters and decay matrix elements in lattice QCD.

The outline of the paper is as follows. In section 2 the necessary details concerning the two-folded sine-Gordon model are introduced. Section 3 presents the formalism of finite size form factors, first the description valid to all orders in  $1/L$  and then determining the leading exponential corrections a.k.a. the  $\mu$ -terms. The theoretical results presented here are compared to numerical data extracted from TCSA in section 4. Section 5 discusses the relevance of these findings to the description of resonances, and in section 6 the conclusions are formulated. The detailed and rather bulky formulae for the exact form factors (determined from the bootstrap) are summarized in Appendix A.

## 2 The two-folded sine-Gordon model in finite volume

The classical action of sine-Gordon theory is

$$\mathcal{A} = \int d^2x \left( \frac{1}{2} \partial_\mu \Phi \partial^\mu \Phi + \frac{m_0^2}{\beta^2} \cos \beta \Phi \right) \quad (2.1)$$

A useful representation of the model at quantum level is to consider it as the conformal field theory of a free massless boson perturbed by a relevant operator. In this framework, the Hamiltonian can be written as

$$H = \int dx \frac{1}{2} : (\partial_t \Phi)^2 + (\partial_x \Phi)^2 : - \lambda \int dx : \cos \beta \Phi : \quad (2.2)$$

where the semicolon denotes normal ordering in terms of the modes of the  $\lambda = 0$  massless field. Due to anomalous dimension of the normal ordered cosine operator, the coefficient

$\lambda$  has dimension

$$\lambda \sim [\text{mass}]^{2-\beta^2/4\pi}$$

and it sets the mass scale of the model. The genuine coupling constant is  $\beta$  which for later convenience is reparametrized as

$$\xi = \frac{\beta^2}{8\pi - \beta^2}$$

The spectrum consists of a doublet of solitons and their bound states, which are called breathers. The scattering amplitudes of this model are briefly reviewed in Appendix A.1. As usual in two-dimensional kinematics, the on-shell energy-momentum two-vector  $(E, p)$  of a particle with mass  $m$  is parametrized with the rapidity  $\theta$ :

$$E = m \cosh \theta \quad , \quad p = m \sinh \theta$$

Lorentz boosts correspond to shifting all rapidities by the same constant.

In finite volume, it is possible to choose quasi-periodic boundary conditions for the field leading to a set of possible local theories labeled by an integer  $k$  called the folding number [15]. To define the  $k$ -folded theory  $SG(\beta, k)$  we take the sine-Gordon field  $\Phi$  as an angular variable with the period

$$\Phi \sim \Phi + \frac{2\pi}{\beta} k \tag{2.3}$$

When the space is a finite circle with circumference (in this case also the volume)  $L$ , i.e.  $x \sim x + L$ , this implies the following quasi-periodic boundary condition for the field

$$\Phi(x + L, t) = \Phi(x, t) + \frac{2\pi}{\beta} km, \quad m \in \mathbb{Z} \tag{2.4}$$

The classical ground states are easily obtained:

$$\Phi = \frac{2\pi}{\beta} n, \quad n = 0, \dots, k - 1 \tag{2.5}$$

which shows that the condition (2.3) corresponds to identifying the minima of the cosine potential with a period  $k$ . In the infinite volume ( $L = \infty$ ) quantum theory these correspond to vacuum states  $|n\rangle$  which have the property

$$\langle n | \Phi(x, t) | n \rangle = \frac{2\pi}{\beta} n \quad n = 0, 1, \dots, k - 1 \tag{2.6}$$

These states are all degenerate in the classical theory and also at quantum level when  $L = \infty$ ; however, tunneling lifts the degeneracy in finite volume  $L < \infty$ . The spectrum of breather multi-particle states is obtained in  $k$  copies corresponding to the  $k$  vacua, and in finite volume tunneling splits the degeneracy between these states by an amount of order  $e^{-ML}$  where  $M$  is the soliton mass. In the  $k$ -folded model, the local operators of most interest are the exponential fields

$$e^{i\frac{n}{k}\beta\Phi} \quad n \in \mathbb{Z}$$

In the sequel the value of  $k$  is set to 2 so the model considered is the 2-folded sine-Gordon theory  $SG(\beta, 2)$ .

### 3 Form factors in finite volume

#### 3.1 Corrections to all order in $1/L$

In this work we restrict our attention to states containing only breathers (i.e. no solitons). As breathers are singlets and therefore scatter diagonally, the formulae derived by Pozsgay and Takács in [12, 13] are directly applicable. The first ingredient is to describe the multi-breather energy levels corresponding to the states

$$|B_{r_1}(\theta_1) \dots B_{r_N}(\theta_N)\rangle$$

whose finite volume counter part we are going to label

$$|\{I_1, \dots, I_N\}\rangle_{r_1 \dots r_N, L}$$

where the  $I_k$  are the momentum quantum numbers. In a finite volume  $L$ , momentum quantization is governed (up to corrections decreasing exponentially with  $L$ ) by the Bethe-Yang equations:

$$Q_k(\theta_1, \dots, \theta_n) = m_{r_k} L \sinh \theta_k + \sum_{j \neq k} \delta_{r_j r_k} (\theta_k - \theta_j) = 2\pi I_k \quad I_k \in \mathbb{Z} \quad (3.1)$$

where the phase-shift is defined as

$$S_{rs}(\theta) = e^{i\delta_{sr}(\theta)}$$

These equations are nothing else than an appropriate extension of the description of two-particle scattering states in finite volume [17, 18]. In general quantum field theories this description is only valid under the inelastic threshold, but due to integrability it can be extended to all multi-particle states regardless of their energy.

In practical calculations, because breathers of the same species satisfy an effective exclusion rule due to

$$S_{rr}(0) = -1$$

it is best to redefine phase-shifts corresponding to them by extracting a minus sign:

$$S_{rr}(\theta) = -e^{i\delta_{rr}(\theta)}$$

so that  $\delta_{sr}(0) = 0$  can be taken for all  $s, r$  and all the phase-shifts can be defined as continuous functions over the whole real  $\theta$  axis. This entails shifting appropriate quantum numbers  $I_k$  to half-integer values. Given a solution  $\tilde{\theta}_1, \dots, \tilde{\theta}_N$  to the quantization relations (3.1) the energy and the momentum of the state can be written as

$$\begin{aligned} E &= \sum_{k=1}^N m_{r_k} \cosh \tilde{\theta}_k \\ P &= \sum_{k=1}^N m_{r_k} \sinh \tilde{\theta}_k = \frac{2\pi}{L} \sum_k I_k \end{aligned}$$

(using that – with our choice of the phase-shift functions – unitarity entails  $\delta_{sr}(\theta) + \delta_{rs}(-\theta) = 0$ ). The rapidity-space density of  $n$ -particle states can be calculated as

$$\rho_{r_1 \dots r_n}(\theta_1, \dots, \theta_n) = \det \mathcal{J}^{(n)} \quad , \quad \mathcal{J}_{kl}^{(n)} = \frac{\partial Q_k(\theta_1, \dots, \theta_n)}{\partial \theta_l} \quad , \quad k, l = 1, \dots, n \quad (3.2)$$

In infinite volume the matrix elements of local operators between multi-particle states composed of breathers can be expressed in terms of the elementary form factor functions

$$F_{r_1 \dots r_N}^{\mathcal{O}}(\theta_1, \dots, \theta_N) = \langle 0 | \mathcal{O} | B_{r_1}(\theta_1) \dots B_{r_N}(\theta_N) \rangle \quad (3.3)$$

using crossing symmetry

$$\langle B_{s_1}(\theta'_1) \dots B_{s_M}(\theta'_M) | \mathcal{O} | B_{r_1}(\theta_1) \dots B_{r_N}(\theta_N) \rangle = F_{s_M \dots s_1 r_1 \dots r_N}^{\mathcal{O}}(\theta'_M + i\pi, \dots, \theta'_1 + i\pi, \tilde{\theta}_1, \dots, \tilde{\theta}_N) + \text{disconnected contributions} \quad (3.4)$$

where disconnected contributions only arise when there are particles in the two states that have identical quantum numbers and momenta.

In terms of the elementary form factors (3.3), the finite volume matrix elements of local operators between multi-particle states can be written as [12]

$$\begin{aligned} & |_{s_1 \dots s_M} \langle \{I'_1, \dots, I'_M\} | \mathcal{O}(0, 0) | \{I_1, \dots, I_N\} \rangle_{r_1 \dots r_N, L} = \\ & \left| \frac{F_{s_M \dots s_1 r_1 \dots r_N}^{\mathcal{O}}(\tilde{\theta}'_M + i\pi, \dots, \tilde{\theta}'_1 + i\pi, \tilde{\theta}_1, \dots, \tilde{\theta}_N)}{\sqrt{\rho_{r_1 \dots r_N}(\tilde{\theta}_1, \dots, \tilde{\theta}_N) \rho_{s_1 \dots s_M}(\tilde{\theta}'_1, \dots, \tilde{\theta}'_M)}} \right| + O(e^{-\mu L}) \end{aligned} \quad (3.5)$$

which is valid provided there are no disconnected terms. This is essentially the extension of the Lellouch-Lüscher formalism [2] to general multi-particle states. The finite volume quantization relations in (3.1) and the expression of density factors  $\rho$  in (3.2) are specific to the setting of two-dimensional integrable field theories, but the relation (3.5) which states that finite volume matrix elements differ from their infinite volume counterparts by normalization factors given by the square roots of densities of states is generally valid in any quantum field theory (with a nonzero mass gap), as can be seen by considering the way this expression was derived in [12].

Note the absolute values in (3.5) that are necessary to take into account that the finite volume and infinite volume phase conventions differ. In our framework it is known how to compensate for the difference. The finite volume eigenvectors obtained from TCSA can be chosen real, as the Hamiltonian is a real symmetric matrix, and then all matrix elements of exponential operators turn out to be real. On the other hand, apart from the  $i$  factors in (A.3) the only complex function is the minimal two-particle form factor  $f_\xi(\theta)$ , whose phase at a real value of the argument is equal to the square root of the  $S$ -matrix. Therefore the above relation can be rewritten as

$$\begin{aligned} & |_{s_1 \dots s_M} \langle \{I'_1, \dots, I'_M\} | \mathcal{O}(0, 0) | \{I_1, \dots, I_N\} \rangle_{r_1 \dots r_N, L} = \\ & \pm \frac{F_{s_M \dots s_1 r_1 \dots r_N}^{\mathcal{O}}(\tilde{\theta}'_M + i\pi, \dots, \tilde{\theta}'_1 + i\pi, \tilde{\theta}_1, \dots, \tilde{\theta}_N)}{\sqrt{\rho_{r_1 \dots r_N}(\tilde{\theta}_1, \dots, \tilde{\theta}_N) \rho_{s_1 \dots s_M}(\tilde{\theta}'_1, \dots, \tilde{\theta}'_M)}} \times \\ & i^{-(N+M)} \sqrt{\prod_{1 \leq k < l \leq M} S_{s_k s_l}(\tilde{\theta}'_k - \tilde{\theta}'_l) \prod_{1 \leq k < l \leq N} S_{r_k r_l}(\tilde{\theta}_k - \tilde{\theta}_l)} + O(e^{-\mu L}) \end{aligned} \quad (3.6)$$

where the only remaining ambiguity is a sign corresponding to the choice of the branch of the square root (note that this ambiguity is also manifest in the TCSA eigenvectors since demanding their reality does not fix their sign). Note also that the values

$$f_\xi(\theta + i\pi)$$

are real whenever  $\theta$  is real.

Disconnected terms may appear when there are two breathers of the same species in the two states whose rapidities exactly coincide. This can happen in two cases: when the two states are identical, or when there is a particle with exactly zero momentum in both of them [13]. Here we only quote the latter since that is needed for our computations. Defining the function

$$\begin{aligned} & \mathcal{F}_{k,l}(\theta'_1, \dots, \theta'_k | \theta_1, \dots, \theta_l) = \\ & \lim_{\epsilon \rightarrow 0} F_{\underbrace{11\dots 1}_{2k+2l+2}}(i\pi + \theta'_1 + \epsilon, \dots, i\pi + \theta'_k + \epsilon, i\pi - \theta'_k + \epsilon, \dots, i\pi - \theta'_1 + \epsilon, i\pi + \epsilon, \\ & 0, \theta_1, \dots, \theta_l, -\theta_l, \dots, -\theta_1) \end{aligned} \quad (3.7)$$

one can write

$$\begin{aligned} & \underbrace{11\dots 1}_{2k+1} \langle \{I'_1, \dots, I'_k, 0, -I'_k, \dots, -I'_1\} | \Phi | \{I_1, \dots, I_l, 0, -I_l, \dots, -I_1\} \rangle_{\underbrace{11\dots 1, L}_{2l+1}} \quad (3.8) \\ & \left( \mathcal{F}_{k,l}(\tilde{\theta}'_1, \dots, \tilde{\theta}'_k | \tilde{\theta}_1, \dots, \tilde{\theta}_l) + mL F_{\underbrace{11\dots 1}_{2k+2l}}(i\pi + \tilde{\theta}'_1, \dots, i\pi - \tilde{\theta}'_1, \tilde{\theta}_1, \dots, -\tilde{\theta}_1) \right) \\ = & \frac{\sqrt{\rho_{2k+1}(\tilde{\theta}'_1, \dots, \tilde{\theta}'_k, 0, -\tilde{\theta}'_k, \dots, -\tilde{\theta}'_1) \rho_{2l+1}(\tilde{\theta}_1, \dots, \tilde{\theta}_l, 0, -\tilde{\theta}_l, \dots, -\tilde{\theta}_1)}}{\text{(phase factor)} + O(e^{-\mu L})} \times \end{aligned}$$

where the compensating phase factor is entirely analogous to the one in (3.6).

The above predictions for finite volume energy levels and matrix elements are expected to be exact to all (finite) orders in  $1/L$  [12, 13] (note that the exponential corrections are non-analytic in this variable).

## 3.2 $\mu$ -terms: the leading exponential corrections

### 3.2.1 $\mu$ -terms for energy levels

Using the ideas in [14], we can model a finite volume  $B_2$  state as a pair of  $B_1$  particles with complex conjugate rapidities

$$B_2(\theta) \sim B_1(\theta + iu)B_1(\theta - iu)$$

where  $u$  can be obtained by solving the  $B_1B_1$  Bethe-Yang equations (written here in exponential form):

$$e^{im_1L \sinh(\theta \pm iu)} S_{11}(\pm 2iu) = 1 \quad (3.9)$$

where

$$S_{11}(\theta) = \frac{\sinh \theta + i \sin \pi \xi}{\sinh \theta - i \sin \pi \xi}$$

The solution for  $u$  has the large volume behavior

$$u \sim \frac{\pi \xi}{2} + \tan \frac{\pi \xi}{2} e^{-\mu_{11}^2 L \cosh \theta} \quad (3.10)$$

with

$$\mu_{11}^2 = \sqrt{m_1^2 - \frac{m_2^2}{4}} = m_1 \sin \frac{\pi \xi}{2}$$

Therefore, for  $L \rightarrow \infty$  one obtains the usual bootstrap identification

$$B_2(\theta) \simeq B_1(\theta + i\pi\xi/2)B_1(\theta - i\pi\xi/2)$$

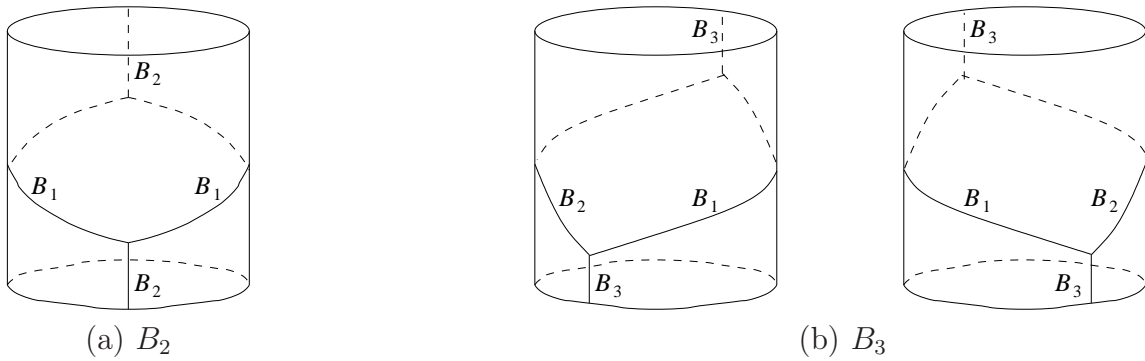


Figure 3.1:  $\mu$ -term diagrams

and the momentum and energy of the state tends to

$$\begin{aligned} m_1 \sinh(\theta + iu) + m_1 \sinh(\theta - iu) &= 2m_1 \cos u \sinh \theta \xrightarrow{L \rightarrow \infty} m_2 \sinh \theta \\ m_1 \cosh(\theta + iu) + m_1 \cosh(\theta - iu) &= 2m_1 \cos u \cosh \theta \xrightarrow{L \rightarrow \infty} m_2 \cosh \theta \end{aligned}$$

where

$$m_2 = 2m_1 \cos \frac{\pi\xi}{2}$$

is the mass of  $B_2$  in terms of that of  $B_1$ , consistent with (A.2). For a stationary  $B_2$ , the energy dependence on the volume is

$$E_2(L) = 2m_1 \cos u \sim m_2 - (\gamma_{11}^2)^2 \mu_{11}^2 e^{-\mu_{11}^2 L} + \dots \quad (3.11)$$

where the second expression shows the asymptotic behavior valid for large enough  $L$ . One can also write

$$\mu_{11}^2 = m_1 \sin u_{12}^1$$

where the  $B_1 B_2 \rightarrow B_1$  fusion angle is

$$u_{12}^1 = \pi \left( 1 - \frac{\xi}{2} \right)$$

The asymptotic behaviour in (3.11) coincides with that predicted by Lüscher's finite volume mass formula [19], which was worked out in more detail for 2-dimensional quantum field theory in [20] and is illustrated graphically in Fig. 3.1 (a). Here  $\gamma_{11}^2$  is the three-particle coupling defined in (A.8). The kinematical variables can be represented by the mass triangle shown in Fig. 3.2, with  $\mu_{ab}^c$  being the height of the triangle perpendicular to the side  $m_c$ . Note that  $\mu_{ab}^c$  can be much smaller than other mass scales in the theory if the binding energy is low, i.e. when  $m_c \sim m_a + m_b$ .

A stationary third breather  $B_3$  can be modeled as a composite of three  $B_1$  particles

$$B_3(\theta = 0) \sim B_1(iu)B_1(0)B_1(-iu)$$

where the (nontrivial) Bethe-Yang equations read

$$e^{im_1 L \sinh(\pm iu)} S_{11}(\pm iu) S_{11}(\pm 2iu) = 1 \quad (3.12)$$

leading to the asymptotic expression

$$u \sim \pi\xi + \frac{4 \sin \pi\xi + 2 \tan \pi\xi}{2 \cos \pi\xi - 1} e^{-m_1 L \sin \pi\xi} \quad (3.13)$$

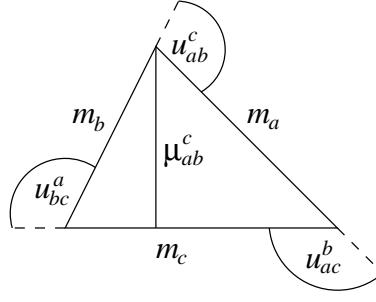


Figure 3.2: Mass triangle, fusion angles and  $\mu$  parameter

The energy of the  $B_3$  level then becomes

$$E_3(L) = m_1(1 + 2 \cos u) \sim m_3 - 2 (\gamma_{12}^3)^2 \mu_{12}^3 e^{-\mu_{12}^3 L} + \dots \quad (3.14)$$

where the three-particle coupling  $\gamma_{12}^3$  is defined in (A.8) and

$$\mu_{12}^3 = m_1 \sin u_{13}^2 = m_2 \sin u_{23}^1$$

with the fusion angles

$$u_{13}^2 = \pi(1 - \xi) \quad u_{23}^1 = \pi \left( 1 - \frac{\xi}{2} \right)$$

The asymptotic behavior in (3.14) is again consistent with the expression given by Lüscher [19, 20], the factor of 2 is due to the presence of two processes contributing the same amount as shown in Fig. 3.1 (b).

### 3.2.2 $\mu$ -term corrections for the form factors

Using the results of [14], these can be computed by continuing (3.6) to complex rapidities that correspond to representing  $B_2$  and  $B_3$  as composites made out of  $B_1$ . One obtains for vacuum- $B_2$  matrix elements the form

$$\langle 0 | \mathcal{O}(0, 0) | \{I\} \rangle_{2,L} = \pm \frac{\sqrt{S_{11}(2i\tilde{u})} F_{11}^{\mathcal{O}}(\tilde{\theta} - i\tilde{u}, \tilde{\theta} + i\tilde{u})}{\sqrt{\rho_{11}(\tilde{\theta} + i\tilde{u}, \tilde{\theta} - i\tilde{u})}} + \dots \quad (3.15)$$

where  $\tilde{\theta}$ ,  $\tilde{u}$  is the solution of (3.9) with the correct momentum, i.e.

$$m_1 L \sinh(\tilde{\theta} + i\tilde{u}) + m_1 L \sinh(\tilde{\theta} - i\tilde{u}) = 2\pi I$$

and the dots denote further (and generally much smaller) exponential corrections; the  $\pm$  sign accounts for the remaining phase ambiguity from the square root. One can similarly evaluate  $B_1 - B_2$  and  $B_1 B_1 - B_2$  matrix elements using

$$\begin{aligned} {}_1 \langle \{I'\} | \mathcal{O}(0, 0) | \{I\} \rangle_{2,L} &= \pm i \frac{\sqrt{S_{11}(2i\tilde{u})} F_{111}^{\mathcal{O}}(i\pi + \tilde{\theta}', \tilde{\theta} - i\tilde{u}, \tilde{\theta} + i\tilde{u})}{\sqrt{m_1 L \cosh \tilde{\theta}' \rho_{11}(\tilde{\theta} + i\tilde{u}, \tilde{\theta} - i\tilde{u})}} + \dots \quad (3.16) \\ {}_{11} \langle \{I'_1, I'_2\} | \mathcal{O}(0, 0) | \{I\} \rangle_{2,L} &= \pm \left[ \frac{\sqrt{S_{11}(2i\tilde{u})} S_{11}(\tilde{\theta}'_1 - \tilde{\theta}'_2)}{\sqrt{\rho_{11}(\tilde{\theta}'_1, \tilde{\theta}'_2) \rho_{11}(\tilde{\theta} + i\tilde{u}, \tilde{\theta} - i\tilde{u})}} \times \right. \\ &\quad \left. F_{1111}^{\mathcal{O}}(i\pi + \tilde{\theta}'_2, i\pi + \tilde{\theta}'_1, \tilde{\theta} - i\tilde{u}, \tilde{\theta} + i\tilde{u}) \right] + \dots \end{aligned}$$



For large enough  $L$ , we can use (3.10) and keep the leading term of these expressions in the limit  $\tilde{u} \rightarrow \pi\xi/2$  to obtain

$$\begin{aligned}
\langle 0|\mathcal{O}(0,0)|\{I\}\rangle_{2,L} &= \pm \frac{F_2^\mathcal{O}(\tilde{\theta})}{\sqrt{m_2 L \cosh \tilde{\theta}}} + O\left(e^{-\mu_{11}^2 L}\right) \\
{}_1\langle\{I'\}|\mathcal{O}(0,0)|\{I\}\rangle_{2,L} &= \pm i \frac{F_{12}^\mathcal{O}(i\pi + \tilde{\theta}', \tilde{\theta})}{\sqrt{m_1 L \cosh \tilde{\theta}' m_2 L \cosh \tilde{\theta}}} + O\left(e^{-\mu_{11}^2 L}\right) \\
{}_{11}\langle\{I'_1, I'_2\}|\mathcal{O}(0,0)|\{I\}\rangle_{2,L} &= \pm \frac{\sqrt{S_{11}(\tilde{\theta}'_1 - \tilde{\theta}'_2)} F_{12}^\mathcal{O}(i\pi + \tilde{\theta}'_2, i\pi + \tilde{\theta}'_1, \tilde{\theta})}{\sqrt{\rho_{11}(\tilde{\theta}'_1 - \tilde{\theta}'_2) m_2 L \cosh \tilde{\theta}}} \times \\
&\quad + O\left(e^{-\mu_{11}^2 L}\right)
\end{aligned} \tag{3.17}$$

where we also used (A.7). This is just what we obtain from the general expression (3.6). In performing this calculation, the singular behavior of the factor  $S_{11}(2i\tilde{u})$  for  $\tilde{u} \rightarrow \pi\xi/2$  is canceled by a singular term from the denominator factor

$$\rho_{11}(\tilde{\theta} + i\tilde{u}, \tilde{\theta} - i\tilde{u}) = \frac{m_2 L \cosh \tilde{\theta}}{2\left(\tilde{u} - \frac{\pi\xi}{2}\right)} + \text{regular terms}$$

For matrix elements involving a stationary  $B_3$  we obtain

$$\begin{aligned}
\langle 0|\mathcal{O}(0,0)|\{0\}\rangle_{3,L} &= \pm i \frac{\sqrt{S_{11}(2i\tilde{u})} S_{11}(i\tilde{u}) F_{111}^\mathcal{O}(-i\tilde{u}, 0, +i\tilde{u})}{\sqrt{\rho_{111}(+i\tilde{u}, 0, -i\tilde{u})}} + \dots \\
{}_1\langle\{I'\}|\mathcal{O}(0,0)|\{0\}\rangle_{3,L} &= \pm \frac{\sqrt{S_{11}(2i\tilde{u})} S_{11}(i\tilde{u}) F_{1111}^\mathcal{O}(i\pi + \tilde{\theta}', -i\tilde{u}, 0, +i\tilde{u})}{\sqrt{m_1 L \cosh \tilde{\theta}' \rho_{111}(+i\tilde{u}, 0, -i\tilde{u})}} + \dots \\
{}_{11}\langle\{I'_1, I'_2\}|\mathcal{O}(0,0)|\{0\}\rangle_{3,L} &= \pm i \left[ \frac{\sqrt{S_{11}(2i\tilde{u})} S_{11}(\tilde{\theta}'_1 - \tilde{\theta}'_2) S_{11}(i\tilde{u})}{\sqrt{\rho_{11}(\tilde{\theta}'_1, \tilde{\theta}'_2) \rho_{111}(+i\tilde{u}, 0, -i\tilde{u})}} \times \right. \\
&\quad \left. F_{11111}^\mathcal{O}(i\pi + \tilde{\theta}'_2, i\pi + \tilde{\theta}'_1, -i\tilde{u}, 0, +i\tilde{u}) \right] + \dots
\end{aligned} \tag{3.18}$$

where  $\tilde{u}$  solves (3.12) with the asymptotics (3.13). There is an exception to the second formula, however: when  $I' = 0$ , the  $B_1$  is stationary and there is a disconnected piece, which according to (3.8) leads to the modification

$${}_1\langle\{0\}|\mathcal{O}(0,0)|\{0\}\rangle_{3,L} = \pm \frac{\sqrt{S_{11}(2i\tilde{u})} S_{11}(i\tilde{u}) \bar{\mathcal{F}}_{1,3}^\mathcal{O}(-i\tilde{u}) + m_1 L \sqrt{S_{11}(2i\tilde{u})} F_{11}^\mathcal{O}(-i\tilde{u}, +i\tilde{u})}{\sqrt{m_1 L \cosh \tilde{\theta}' \rho_{111}(+i\tilde{u}, 0, -i\tilde{u})}} + \dots \tag{3.19}$$

where

$$\bar{\mathcal{F}}_{1,3}^\mathcal{O}(\tilde{\theta}) = \lim_{\epsilon \rightarrow 0} F_{1111}^\mathcal{O}(i\pi + \epsilon, \tilde{\theta}, 0, -\tilde{\theta})$$

Using the exchange property

$$\begin{aligned}
F_{i_1 \dots i_k i_{k+1} \dots i_n}^\mathcal{O}(\theta_1, \dots, \theta_k, \theta_{k+1}, \dots, \theta_n) = \\
S_{i_k i_{k+1}}(\theta_k - \theta_{k+1}) F_{i_1 \dots i_{k+1} i_k \dots i_n}^\mathcal{O}(\theta_1, \dots, \theta_{k+1}, \theta_k, \dots, \theta_n)
\end{aligned} \tag{3.20}$$

we can write

$$\begin{aligned}\bar{\mathcal{F}}_{1,3}^{\mathcal{O}}(\tilde{\theta}) &= S(-\tilde{\theta})\mathcal{F}_{1,3}^{\mathcal{O}}(\tilde{\theta}) \\ \text{where } \mathcal{F}_{1,3}^{\mathcal{O}}(\tilde{\theta}) &= \lim_{\epsilon \rightarrow 0} F_{1111}^{\mathcal{O}}(i\pi + \epsilon, 0, \tilde{\theta}, -\tilde{\theta})\end{aligned}$$

which explains the presence of the factor  $S_{11}(i\tilde{u})$  in the coefficient of  $\bar{\mathcal{F}}_{1,3}^{\mathcal{O}}$  in (3.19), in contrast to formula (3.8). (The factor  $\sqrt{S_{11}(2i\tilde{u})}$ , common to both terms results from the analytic continuation of the compensating phase factors discussed in the previous subsection, as all similar factors in other cases do as well.)

It can again be verified that for  $L$  large enough, taking the limit  $\tilde{u} \rightarrow \pi\xi$  again results in agreement with what is expected from (3.6):

$$\begin{aligned}\langle 0|\mathcal{O}(0,0)|\{0\}\rangle_{3,L} &= \pm \frac{F_3^{\mathcal{O}}(0)}{\sqrt{m_3 L}} + O\left(e^{-\mu_{12}^3 L}\right) \\ {}_1\langle\{I'\}|\mathcal{O}(0,0)|\{0\}\rangle_{3,L} &= \pm i \frac{F_{13}^{\mathcal{O}}(i\pi + \tilde{\theta}', 0)}{\sqrt{m_1 L \cosh \tilde{\theta}' m_3 L}} + O\left(e^{-\mu_{12}^3 L}\right) \\ {}_{11}\langle\{I'_1, I'_2\}|\mathcal{O}(0,0)|\{0\}\rangle_{3,L} &= \pm \frac{\sqrt{S_{11}(\tilde{\theta}'_1 - \tilde{\theta}'_2)} F_{13}^{\mathcal{O}}(i\pi + \tilde{\theta}'_2, i\pi + \tilde{\theta}'_1, 0)}{\sqrt{\rho_{11}(\tilde{\theta}'_1 - \tilde{\theta}'_2) m_3 L}} \times \\ &\quad + O\left(e^{-\mu_{12}^3 L}\right)\end{aligned}\tag{3.21}$$

Note that the additional term in (3.19) drops out because the factor  $S_{11}(2i\tilde{u})$  has no pole to compensate for the singular behavior of the denominator which is of the form

$$\rho_{111}(+i\tilde{u}, 0, -i\tilde{u}) \sim \frac{m_3 L}{(\tilde{u} - \pi\xi)^2} + \text{less singular terms}$$

### 3.3 Beyond the leading $\mu$ -terms

It is important to consider subleading exponential corrections. First of all, the breathers also have  $\mu$ -terms corresponding to their description as soliton-antisoliton bound states, with the characteristic scale

$$\mu_{s\bar{s}}^k = \sqrt{M^2 - \frac{m_k^2}{4}}$$

In addition to the  $\mu$ -terms there are corrections which correspond to particle loops winding around the space-time cylinder. They are called  $F$ -terms because they depend on the forward scattering amplitude  $F$  continued to rapidity difference with imaginary part  $i\pi/2$  [19] and are suppressed by the mass of the particle propagating in the loop. Last, but not least, there are also the tunneling corrections related to the presence of multiple vacua ( $k = 2$  in the case considered below), suppressed by the soliton mass  $M$ , which are essentially vacuum versions of  $F$ -terms. These contributions were evaluated using the dilute instanton gas approximation in [15].  $F$ -terms contributions are illustrated in Fig. and their scales are compared explicitly to  $\mu$ -term scales at the beginning of the next section.

## 4 Determining matrix elements of local operators: the effect of $\mu$ -terms

To evaluate the form factors numerically, we use the truncated conformal space approach (TCSA) pioneered by Yurov and Zamolodchikov [10]. The essential idea is to truncate

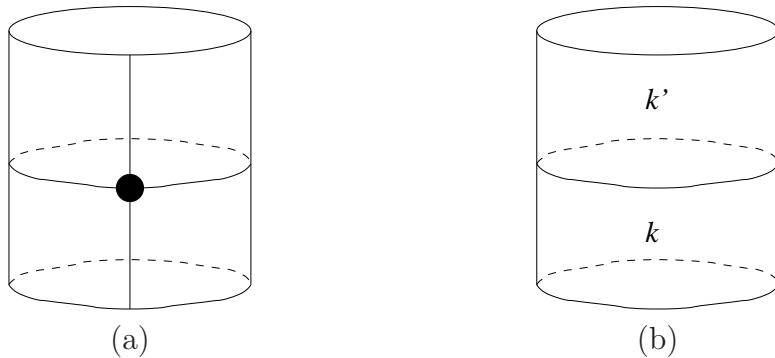


Figure 3.3: (a)  $F$ -term correction to the mass, the filled circle denotes the forward scattering amplitude evaluated at  $\theta + i\pi/2$ , where  $\theta$  is the rapidity of the particle propagating in the loop.

(b) Vacuum tunneling between two adjacent vacua ( $k' = k \pm 1$ ), the loop is the world line of a soliton propagating around the cylinder.

the Hilbert space of the massless free boson introducing an upper energy cutoff (called the truncation), which gives a finite dimensional space in finite volume  $L$ . The Hamiltonian (2.2) can then be represented as a finite numerical matrix and the energy levels evaluated by numerical diagonalization. Truncation introduces a source of systematic errors, known as truncation errors, which are analogous to discretization errors in lattice field theory. Since the wave-functions of the the interacting theory are expanded in terms of lowest-lying states of the limiting conformal model (obtained as the high energy limit  $L \rightarrow 0$ ), truncation errors grow with volume and they are also larger for higher lying levels. In most of the calculations in this paper they are too small to be considered, with the exception of the issue of resonances treated in section 5.

The extension of TCSA to the sine-Gordon model was developed in [21] and has found numerous applications since then. The Hilbert space can be split by the eigenvalues of the topological charge  $\mathcal{Q}$  (or winding number) and the spatial momentum  $P$ , where the eigenvalues of the latter are of the form

$$\frac{2\pi s}{L} \quad s \in \mathbb{Z}$$

In sectors with vanishing topological charge, we can make use of the symmetry of the Hamiltonian under

$$\mathcal{C} : \quad \Phi(x, t) \rightarrow -\Phi(x, t)$$

which is equivalent to conjugation of the topological charge. The truncated space can be split into  $\mathcal{C}$ -even and  $\mathcal{C}$ -odd subspaces that have roughly equal dimensions, which speeds up the diagonalization of the Hamiltonian.

Using relation (A.6) we can express all energy levels and matrix elements in units of (appropriate powers of) the soliton mass  $M$ , and we also introduce the dimensionless volume variable  $l = ML$ . The general procedure is the same as in [12, 13]: the particle content of energy levels can be identified by matching the numerical TCSA spectrum against the predictions of the Bethe-Yang equations (3.1). After identification, one can compare the appropriate matrix elements to the theoretical values given by (3.5).

A detailed study of breather form factors based on the formalism explained in subsection 3.1 has been already performed in [16], therefore it is not repeated here. For the sake of concentrating on the essence of the matter, the effect of  $\mu$ -terms is demonstrated on selected examples. In the process of the computation, the analysis was performed for a large number of different matrix elements and also for several values of coupling constant  $\xi$ , so the data

shown are just a small, but representative subset of results. In view of the next section (dealing with resonances) the most interesting operator to study is

$$\mathcal{O} = e^{i\frac{\beta}{2}\Phi(0)}$$

to which therefore all the form factor plots correspond. The numerical data presented below correspond to the coupling  $\xi = 50/311$ , for which it is instructive to compare the scales involved. The masses of the first three breathers in terms of the soliton mass  $M$  are

$$\begin{aligned} m_1 &= 0.49973 \cdots \times M \\ m_2 &= 0.96775 \cdots \times M \\ m_3 &= 1.37439 \cdots \times M \end{aligned}$$

The  $\mu$ -term scales are

$$\begin{aligned} \mu_{11}^2 &= 0.12486 \cdots \times M \\ \mu_{12}^3 &= 0.24181 \cdots \times M \\ \mu_{s\bar{s}}^1 &= 0.96828 \cdots \times M \\ \mu_{s\bar{s}}^2 &= 0.87514 \cdots \times M \\ \mu_{s\bar{s}}^3 &= 0.72647 \cdots \times M \end{aligned}$$

Therefore it can be seen that the leading exponential corrections are those driven by the splittings  $B_2 \rightarrow B_1 B_1$  and  $B_3 \rightarrow B_1 B_2$ , which are exactly the ones described by the considerations in subsection 3.2. It is also meaningful to beyond the leading asymptotics to evaluate them (i.e. to consider the full solution of the associated Bethe-Yang equations), because even  $4\mu_{11}^2$  and  $2\mu_{12}^3$  are smaller than the next scale  $m_1$  (although the latter only slightly for this particular value of the coupling).

## 4.1 Finite volume mass corrections

One can start by checking whether the mass corrections predicted by eqns. (3.11) for  $B_2$  and (3.14) for  $B_3$  states agree with the numerical energy levels extracted from TCSA. Note that there are two copies of zero-momentum  $B_2$  and  $B_3$  levels in a 2-folded model, so the relevant question is whether the finite volume mass gaps evaluated from both of them agrees with a single  $\mu$ -term correction, at least for volumes that are large enough for higher exponential terms to be negligible. Indeed, Fig. 4.1 demonstrates that it is so. The dashed line shows the infinite volume mass value, while the continuous one is the  $\mu$ -term corrected behavior. The discrete dots show the two mass gaps measured in TCSA.

Note that the correction is rather small (of the order of at most a few percent) for  $ML > 10$ . Since the smallest particle mass for the coupling considered is

$$m_1 = 2M \sin \frac{\pi\xi}{2} \approx 0.5M$$

this corresponds to volumes larger than five times the correlation length of the model. According to the considerations in [2], this should be enough to neglect these corrections in practical computations (in QCD the role of  $m_1$  is played by the pion mass  $m_\pi$ ).

## 4.2 Vacuum–one-particle matrix elements

For these matrix elements, we plot the dimensionless quantity

$$f_k(L) = M^{-x} \sqrt{m_k L} \langle 0 | \mathcal{O} | \{0\} \rangle_{k,L} \quad (4.1)$$

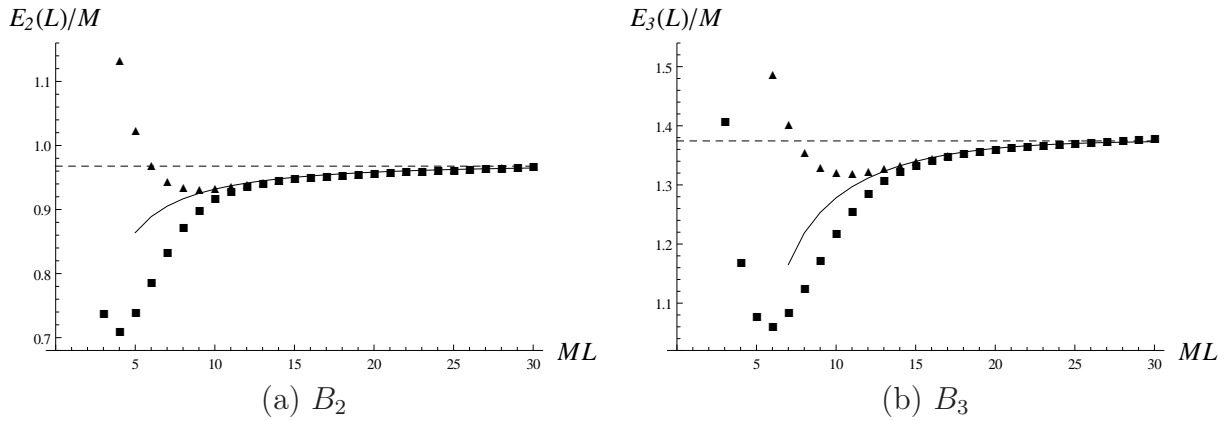


Figure 4.1:  $\mu$ -term corrections for finite volume mass at  $\xi = 50/311$

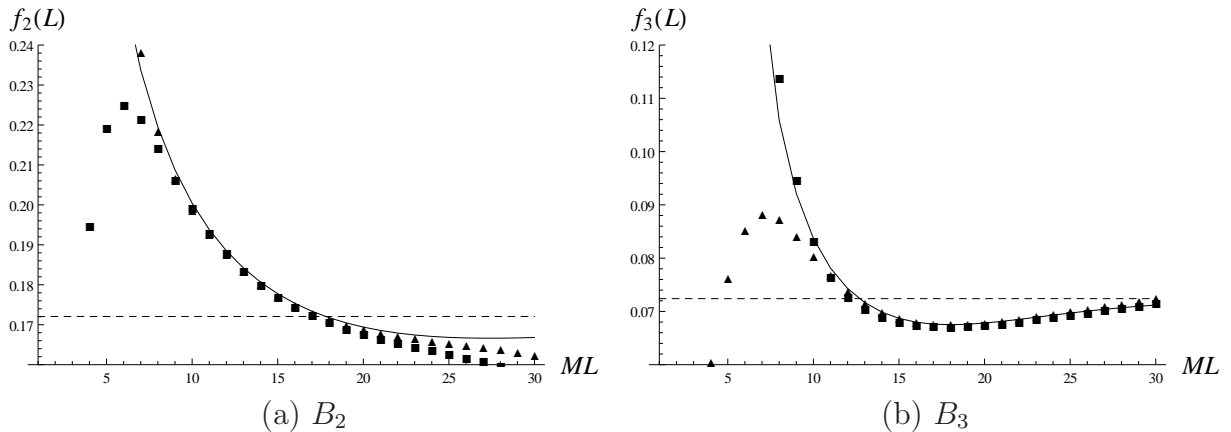


Figure 4.2:  $\mu$ -term corrections to the vacuum–one-particle matrix element at  $\xi = 50/311$ . In each case, the dashed line shows the constant behavior expected when neglecting exponential corrections, the continuous line is the one including the  $\mu$ -term corrections, while the TCSA matrix elements are represented by the two sets of discrete data points.

where

$$x = \frac{\beta^2}{16\pi} = \frac{\xi}{2(1 + \xi)}$$

is the exact scaling dimension of the operator  $\mathcal{O}$ . Using formula (3.5) this is naively expected to be constant

$$f_k(L) = M^{-x} F_k^{\mathcal{O}}(0) + O(e^{-\mu L}) \quad (4.2)$$

where

$$F_k^{\mathcal{O}}(\theta) = \langle 0 | \mathcal{O} | B_k(\theta) \rangle$$

is the appropriate infinite volume form factor (which is eventually independent of  $\theta$  due to Lorentz invariance). As demonstrated by Fig. 4.2, however, the exponential corrections predicted by (3.15) and the first equation in (3.18), coming from the bound state structure of  $B_2$  and  $B_3$  lead to observable deviations from this behavior, which agrees quite well with the numerical results. Still, one could say that in the regime  $ML > 10$  these are expected to be less than 10%, and their presence can be detected from the fact that  $f_k(L)$  is not constant. Note that for each  $k$ , there are two one-particle  $B_k$  states, and with the two vacua this gives four possible matrix elements. However, two of these are very small due to suppression by tunneling.

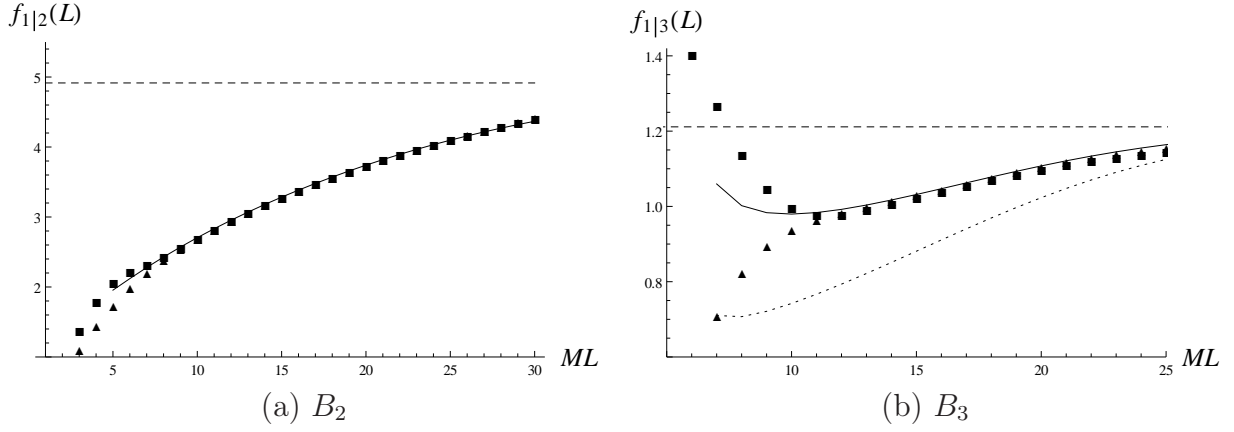


Figure 4.3:  $\mu$ -term corrections to the one-particle–one-particle matrix element at  $\xi = 50/311$

### 4.3 One-particle–one-particle matrix elements

Turning now to matrix elements of the form

$$f_{1|k}(L) = M^{-x} \sqrt{m_1 L} \sqrt{m_k L} \langle \{0\} | \mathcal{O} | \{0\} \rangle_{k,L} \quad (4.3)$$

we encounter a surprise. According to (3.5), such matrix elements are expected to equal

$$f_{1|k}(L) = M^{-x} F_{1k}^{\mathcal{O}}(i\pi, 0) + O(e^{-\mu L}) \quad (4.4)$$

where

$$F_{1k}^{\mathcal{O}}(\theta_1, \theta_2) = \langle 0 | \mathcal{O} | B_1(\theta_1) B_k(\theta_2) \rangle$$

which under the crossing property (3.4) entails that

$$f_{1|k}(L) = M^{-x} \langle B_1(0) | \mathcal{O} | B_k(0) \rangle + O(e^{-\mu L})$$

so this function must be approximately equal to a constant. However, it is very obvious from Fig. 4.3 that the exponential corrections are huge (of the order of 100% for  $k = 2$ ) and the constant value (showed by the dashed line) is approached very slowly. It is also apparent that the  $\mu$ -term corrected predictions (the continuous lines) from (3.16) and (3.19) describe the numerical data very well. For the case of  $B_3$  the “naive”  $\mu$ -term prediction from the second equation in (3.18) is also shown with dotted line, demonstrating that it is very important to get the disconnected parts of the  $\mu$ -terms right to achieve agreement.

### 4.4 Two-particle–one-particle matrix elements

Let us now study

$$f_{11|k}(L) = M^{-x} \sqrt{\rho_{11}(\tilde{\theta}, -\tilde{\theta})} \sqrt{m_k L} \langle \{-\frac{1}{2}, \frac{1}{2}\} | \mathcal{O} | \{0\} \rangle_{k,L} \quad (4.5)$$

where  $\tilde{\theta}$  solves the Bethe-Yang equation

$$m_1 L \sinh \theta + \delta_{11}(2\theta) = \frac{1}{2} \quad , \quad \delta_{11}(\theta) = -i \log(-S_{11}(\theta))$$

The expectation from the naive finite-volume formula (3.5) is that

$$f_{11|k}(L) = M^{-x} \left| F_{11k}^{\mathcal{O}}(i\pi - \tilde{\theta}, i\pi + \tilde{\theta}, 0) \right| + O(e^{-\mu L}) \quad (4.6)$$

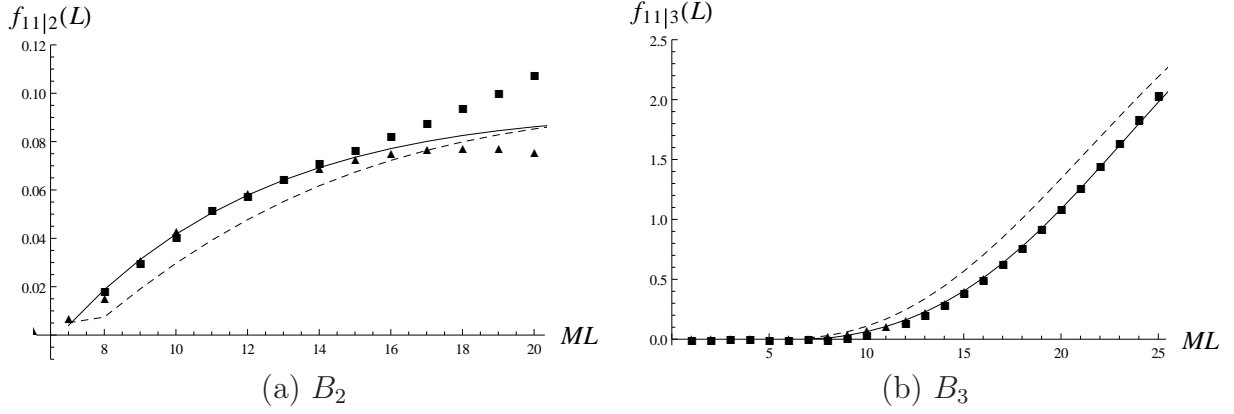


Figure 4.4:  $\mu$ -term corrections to the two-particle–one-particle matrix element at  $\xi = 50/311$ . The observable deviation for  $L \gtrsim 15$  in graph (a) is entirely due to numerical problems: the raw datum determined from TCSA is the matrix element  $\langle \{-\frac{1}{2}, \frac{1}{2}\} | \mathcal{O} | \{0\} \rangle_{2,L}$ , which is so small in this range of the volume that it is of the same magnitude as the truncation error itself.

where

$$F_{11k}^{\mathcal{O}}(\theta_1, \theta_2, \theta_3) = \langle 0 | \mathcal{O} | B_1(\theta_1) B_1(\theta_2) B_k(\theta_3) \rangle$$

Once again, Fig. 4.4 demonstrates that the exponential corrections play an important role, and yield corrections of up to 20-30%. This is very important because using the crossing property (3.4) one can see that the matrix element measured by the functions  $f_{11|k}$  is

$$F_{11k}^{\mathcal{O}}(i\pi - \tilde{\theta}, i\pi + \tilde{\theta}, 0) = \langle B_1(\tilde{\theta}) B_1(-\tilde{\theta}) | \mathcal{O} | B_k(\theta_3) \rangle$$

which for  $k = 3$  drives the decay  $B_3 \rightarrow B_1 B_1$ , under a perturbation by the operator

$$\frac{1}{2i} (\mathcal{O} - \mathcal{O}^\dagger) = \sin \frac{\beta}{2} \Phi$$

Here we made use of the charge conjugation symmetry

$$\mathcal{C} : \quad \Phi(x, t) \rightarrow -\Phi(x, t)$$

of the model which ensures that

$$\langle B_1(\tilde{\theta}) B_1(-\tilde{\theta}) | \mathcal{O}^\dagger | B_3(\theta_3) \rangle = -\langle B_1(\tilde{\theta}) B_1(-\tilde{\theta}) | \mathcal{O} | B_3(\theta_3) \rangle$$

because

$$\mathcal{C} \mathcal{O} \mathcal{C}^{-1} = \mathcal{O}^\dagger \quad \text{for } \mathcal{O} = e^{i\frac{\beta}{2}\Phi}$$

and both  $B_1$  and  $B_3$  are odd under  $\mathcal{C}$ . According to the data in Fig. 4.4, by omitting the  $\mu$ -term contribution we would significantly underestimate the true infinite volume matrix element (the dashed line) on the basis of the TCSA data. Also note that although the decay of  $\mu$ -terms is exponential in the asymptotic regime, in the volume range available in the numerical method it could be so slow as to be practically unobservable as displayed in Fig. 4.4. What is most surprising is the marked contrast to the case of the energy level corrections in Fig. 4.1, which are driven by the same scales  $\mu_{11}^2$  and  $\mu_{12}^3$ .

It is shown in the next section that together with another source of error (also related to the  $\mu$ -terms) this explains the dominant source of systematic error encountered in the case of the  $B_3$  resonance in the two-frequency sine-Gordon model [11].

## 5 Decay widths of resonances in the two-frequency sine-Gordon model

Now we turn to an application of the results in the previous section. Consider the two-frequency sine-Gordon model defined by the Hamiltonian

$$H_{DSG} = \int dx : \frac{1}{2}(\partial_t \Phi)^2 + \frac{1}{2}(\partial_x \Phi)^2 : - \int dx \left( \lambda : \cos \beta \Phi : + \zeta : \sin \frac{\beta}{2} \Phi : \right) \quad (5.1)$$

where normal-ordering is understood treating the field  $\Phi$  as a free massless boson, i.e. the theory is treated as a perturbed conformal field theory similarly to (2.2). One can consider this model to be a perturbation of sine-Gordon field theory by the integrability-breaking coupling  $\zeta$ , and using the exact form factors in the  $\zeta = 0$ , a so-called form factor perturbation theory (FFPT) can be developed [22, 23]. The spectrum and phase structure of this model has been studied extensively in the literature [24, 25, 26, 27, 28, 23]. The integrability breaking interaction can be assigned the dimensionless parameter

$$t = \frac{\zeta}{M^{\frac{4+3\xi}{2+2\xi}}} \quad (5.2)$$

This model can be considered as a toy model for hadrons: the  $\zeta = 0$  theory is in our setting analogous to QCD, with the breathers being the mesons, which in this limit are all stable. Switching on  $\zeta$  makes the mesons unstable, and the ones that are over the threshold  $2m_1$  are allowed to decay. Consider the decay of  $B_3$  which in the rest frame has the kinematics

$$B_3(0) \rightarrow B_1(\theta_c) + B_1(-\theta_c)$$

with the rapidities of the outgoing  $B_1$ s given by energy conservation.

$$2 \cosh(\theta_c) = \frac{m_3}{m_1} = \frac{\sin \frac{3\pi\xi}{2}}{\sin \frac{\pi\xi}{2}}$$

Using form factor perturbation theory, the decay width can be calculated [11]

$$\frac{\Gamma_{3 \rightarrow 11}}{M} = t^2 \frac{s_{311}(\theta_c)^2}{\left(\frac{m_3}{M}\right)^2 \frac{m_1}{M} \sqrt{\left(\frac{m_3}{2m_1}\right)^2 - 1}} \quad (5.3)$$

where the (dimensionless) decay matrix element is given by

$$s_{311}(\theta_c) = \frac{f_{311}(\theta_c)}{M^{\frac{\xi}{2+2\xi}}} \quad \text{where} \quad f_{311}(\theta_c) = |F_{311}^\Psi(i\pi, \theta_c, -\theta_c)| = |F_{311}^\mathcal{O}(i\pi, \theta_c, -\theta_c)|$$

where

$$\Psi = \sin \frac{\beta}{2} \Phi(0) = \frac{1}{2i}(\mathcal{O} - \mathcal{O}^\dagger) \quad \text{with} \quad \mathcal{O} = e^{i\frac{\beta}{2}\Phi(0)}$$

In the previous work [11], the prediction (5.3) was compared to numerical TCSA data. We developed two methods, of which we only consider the so-called ‘‘improved mini-Hamiltonian’’ (imH) method, because it is effectively a direct numerical determination of the decay matrix element  $s_{311}(\theta_c)$  of the perturbing Hamiltonian.

The results are shown in Table 5.1 where we use the following parameter for the sine-Gordon coupling:



$R$	imH	FFPT	$ML_0$
1.5	$1.185 \pm 0.034$	1.1694	12.398
1.6	$0.883 \pm 0.011$	0.9303	11.588
1.7	$0.592 \pm 0.003$	0.6383	11.927
1.9	$0.274 \pm 0.001$	0.2917	13.615
2.2	$0.1046 \pm 0.0002$	0.0999	17.475
2.5	$0.04767 \pm 2 \cdot 10^{-5}$	0.0392	22.309
2.6	$0.03773 \pm 6 \cdot 10^{-5}$	0.0295	24.089
2.7	$0.03022 \pm 5 \cdot 10^{-5}$	0.0224	25.946

Table 5.1: Measured values of  $s_{311}$  using the “improved mini-Hamiltonian” method, compared to the theoretical prediction labeled by FFPT. The last column contains the volume corresponding to the level crossing at zero perturbing coupling. The uncertainties shown are crude estimates of truncation errors from TCSA.

$$R = \frac{\sqrt{4\pi}}{\beta} \quad \Rightarrow \quad \xi = \frac{1}{2R^2 - 1}$$

(the value  $\xi = 50/311$  used in section 4 corresponds to  $R = 1.9$ ).

Notice that the agreement is not particularly good. The errors are estimates of the truncation errors coming from the energy cutoff introduced in TCSA, which is analogous to the lattice spacing in QCD. For  $R > 1.7$  this clearly does not explain the deviation between the numerical and theoretical results. It was already noted in the original paper [11] and it was (correctly) thought to originate from exponential finite size corrections, however at that time the tools to test this hypothesis had not yet been developed.

In subsection 4.4 we already considered this particular matrix element in finite volume and noted that the  $\mu$ -terms did explain the deviation between the naive expectation (3.5) and the TCSA data. To investigate whether this helps in the case of the resonance width determination, we have to correct errors coming from two sources:

1. The position of the crossings between the  $B_3$  and the  $B_1B_1$  levels is not where one naively expects it to be. Neglecting  $\mu$ -terms, this would be at the position where

$$E_{11}(L_0) = m_3 \tag{5.4}$$

with

$$E_{11}(L) = 2m_1 \cosh \tilde{\theta}$$

where  $\tilde{\theta}$  solves

$$m_1 L \sinh \theta + \delta_{11}(\theta) = 2\pi I \tag{5.5}$$

with  $I = 1/2$  for the first two-particle level.

When incorporating the leading  $\mu$ -term correction to the  $B_3$  level, the equation to solve is

$$E_{11}(L) = E_3(L) \tag{5.6}$$

where

$$E_3(L) = m_1(1 + \cos 2\tilde{u})$$

with  $\tilde{u}$  solving (3.12) i.e.

$$e^{im_1 L \sinh(\pm iu)} S_{11}(\pm iu) S_{11}(\pm 2iu) = 1$$

$R$	$ML_0(\text{TCSA})$	$ML_0(\text{without } \mu)$	$ML_0(\text{with } \mu)$
1.5	12.398	11.453	11.699
1.6	11.588	10.534	11.035
1.7	11.927	10.839	11.513
1.9	13.615	12.539	13.446
2.2	17.475	16.312	17.439
2.5	22.309	21.015	22.288
2.6	24.089	22.757	24.068
2.7	25.946	24.582	25.926

Table 5.2: Positions of line-crossings: comparing the measured values and the theoretical results obtained without/with the  $B_3$   $\mu$ -corrections.

$R$	$\mu\text{-imH}$	$s_{311}(\theta_1)$
1.7	0.806(4)	0.868
1.9	0.401(1)	0.401
2.2	0.138	0.134
2.5	0.0528	0.0509
2.6	0.0392	0.0378
2.7	0.0294	0.0285

Table 5.3: Comparing the TCSA results for  $s_{311}$  using the “improved mini-Hamiltonian” method with  $\mu$ -term corrections, compared to the theoretical prediction taken at the modified kinematical point  $\theta_1$  instead of  $\theta_c$ .

The results are displayed in Table 5.2: note that the  $B_3$   $\mu$ -term does explain the position of the level crossing for  $R \gtrsim 1.9$  very well. The remaining discrepancy results from further exponential corrections, both to the  $B_3$  and the  $B_1B_1$  level.

Note that as a result of the difference between (5.4) and (5.6), the rapidity  $\tilde{\theta}$  of the  $B_1$  particles does not equal to  $\theta_c$ , so that means we are not measuring the matrix element at the proper kinematical point. As a result, the matrix element relevant to the comparison is

$$s_{311}(\theta_1)$$

where  $\theta_1$  is the solution of (5.5) at the actual position of the line crossing.

2. The other effect comes from the  $\mu$ -term correction for the volume dependence of the matrix element, which can be determined from the third formula in (3.18). Notice that this requires the knowledge of the five-particle form factor function  $F_{11111}$ . This can be used to correct the result obtained from the “improved mini-Hamiltonian” method.

The end result is summarized in Table 5.3. Notice that the agreement between theory and numerics is improved by an order of magnitude for  $R \gtrsim 1.9$ , to a few percent deviation instead of 10-50 % (the almost exact equality at  $R = 1.9$  is simply a numerical accident).

## 6 Conclusions and outlook

### 6.1 Why are the $\mu$ -terms so large?

The first question to address is: how could the  $\mu$ -terms be so large in the case of one-particle–one-particle and two-particle–one-particle matrix elements? They decay exponentially by the volume, and therefore are expected to decrease very quickly. As a rule of thumb volumes larger than five times the correlation length of the theory are expected to be large enough to safely neglect them when calculating to an accuracy of a few percent. This is borne out by the finite volume mass corrections examined in subsection 4.1. It is important to note that the  $\mu$ -term predictions for the mass corrections read

$$\begin{aligned} E_2(L) &= 2m_1 \cos u_2 \\ E_3(L) &= m_1(1 + 2 \cos u_3) \end{aligned}$$

with

$$\begin{aligned} u_2 &= \frac{\pi\xi}{2} + O(e^{-\mu_{11}^2 L}) \\ u_3 &= \pi\xi + O(e^{-\mu_{12}^3 L}) \end{aligned}$$

Note that these enter as arguments of cosine functions, which are very smooth and have derivatives of order 1. As a result, their contributions are relatively small for  $\mu L > 1$ , with the asymptotic forms

$$\begin{aligned} E_2(L) &= m_2 - (\gamma_{11}^2)^2 \mu_{11}^2 e^{-\mu_{11}^2 L} + \dots \\ E_3(L) &= m_3 - 2 (\gamma_{12}^3)^2 \mu_{12}^3 e^{-\mu_{12}^3 L} + \dots \end{aligned}$$

What about matrix elements then? The great difference in the  $\mu$ -term corrected finite-volume matrix elements (3.15,3.16), (3.18) and (3.19) is that the parameter  $u$  also appears in them as kinematical argument of form factors. When the parameters  $u$  are expanded around their asymptotic value, the correction takes the form of the  $\mu$ -term exponential multiplied by the derivative of the form factor<sup>1</sup>. Form factors, however, can be rapidly varying functions of their arguments. Indeed, they have singularities corresponding to bound states and even in the absence of these they always have disconnected contributions. These disconnected contributions can appear whenever there are particle rapidities displaced by  $i\pi$ , which according to the crossing relation (3.4) corresponds to a matrix elements with one or more particles with identical quantum numbers (including momenta) in the two states between which the matrix elements of the local operator are taken.

The data are indeed consistent with this interpretation. As shown on the example of vacuum–one-particle matrix elements,  $\mu$ -term contributions are similar in magnitude to the mass corrections. There are countless other data generated in previous studies (and also for testing during this work) for matrix elements between vacuum and multi-particle states, and the results are always similar:  $\mu$ -terms appear, but their magnitude is consistent with what is expected from the energy levels. They can only contribute much when their scale  $\mu$  is very small, i.e. for volumes  $\mu L < 1$  (which can still be a headache in some cases, and this provided the motivation for the investigation in [14]).

However, for matrix elements with multi-particle states on both sides one runs a good chance of running into problems with the rapid variation of the form factor appearing in the  $\mu$ -term formulae. Sometimes it is even possible to hit a disconnected piece head-on,

---

<sup>1</sup>We have not written these expansions explicitly; the interested reader can consult [14] for examples.

as happened for the stationary  $B_1$ - $B_3$  matrix element for which the theoretical prediction (3.19) did include an additional term which introduced an additional factor of  $L$  into the volume dependence.

## 6.2 Implications for the determination of matrix elements

When matrix elements are to be determined numerically, whether in lattice QCD or in the TCSEA approach, it is necessary to model the volume dependence of the matrix elements in order to extract the infinite volume result one is interested in. The usual way to model it accounts for the difference in the normalization between the infinite volume and finite volume matrix elements, taken into account by the state density factors in eqn. (3.5). It is important to include the corrections by the scattering between the particles in finite volume (taken into account by the Bethe-Yang equations (3.1)), because these are of order of some inverse power of  $L$ . Indeed, this is what Lellouch and Lüscher do in their work [2]. Exponential finite size corrections, on the other hand, correspond to radiative corrections specific to finite volume where the loop winds around because of the periodic boundary conditions, and are often neglected.

In some cases (notably those involving only stationary particles) the properly normalized matrix elements are predicted to be constant up to exponential finite size corrections. So the presence of such corrections can be observed by the fact that the matrix element is not a constant, as in subsections 4.2 and 4.3. Therefore one could at least have the idea whether there are sizable exponential corrections, and with a bit of luck one may even try to fit it and extrapolate to infinite volume. However, in cases involving moving particles as in subsection 4.4, this does not work: there is no way of telling the qualitative difference between the volume dependence of the dashed and continuous lines in Fig. 4.4 without having a theoretical understanding of the  $\mu$ -terms.

If one tries to determine the infinite volume form factor without accounting for the  $\mu$ -term, one can easily commit a (systematic) error of the order of 20-50% (for most of the parameter space in the examples of two-particle-one-particle form factors considered here), and sometimes even errors of the order of 100% (for the  $B_1 - B_2$  case)!

Therefore the question is whether it is possible to have a theoretical understanding of  $\mu$ -terms. In the case of integrable models the job is made easier by the existence of exact solutions to the form factor bootstrap, in terms of which one can express the  $\mu$ -term contributions by analytically continuing the description (3.6). Note that for the case of  $B_1 B_1 - B_3$  matrix elements, which is of interest to resonances in the two-frequency sine-Gordon model, this requires knowledge of a five-particle form factor, a quite nontrivial object. Therefore this does not seem a viable option in the case of theories like QCD, where the task is to determine weak interaction matrix elements between hadron states.

We remark that  $F$ -term type exponential finite size corrections are essentially perturbative when considered in terms of low energy effective field theory; this is already clear from the derivation of finite volume mass corrections by Lüscher [19]. In lattice QCD, they are handled by using chiral perturbation theory to construct the loop integrals, which are then put into finite volume using the finite volume perturbation theory formalism [29, 30, 31, 32, 33]. The unknown matrix elements entering them are parametrized by some low-energy constants, which are to be determined by fitting to volume dependence numerically obtained on the lattice.

### 6.3 Implications for resonances

For resonances, there is not even the silver lining that existed for matrix elements involving only stationary particles, where one could at least observe if the volume dependence was not quite right. The reason is that their properties can be measured by observing level splittings, which occur at particular values of the volume. Even in the two-dimensional setting, finding two or more level crossings (more properly these are level avoidances) of the same type (meaning the same particle content for the levels) at substantially different values of the volume, and with the numerics accurate enough, is a tough problem [11]. However, to see whether there are substantial exponential finite size corrections to the decay rates one needs to do exactly that: the most straightforward way out is to find level crossings at several different values of the volume, and perform an infinite volume extrapolation, or at least get an estimate for the systematic error caused by the exponential corrections.

### 6.4 Closing remarks

Without having a handle on the size of the exponential finite size corrections one cannot tell whether the observed discrepancy e.g. between a lattice result and an experimentally measured decay width is a result of systematic error or a disagreement between theoretical model and physical reality. Therefore it is important to have a good theoretical description, or at least an estimate of these corrections. One special feature of  $\mu$ -terms is that in contrast to all other exponential corrections which are bounded by the value of the mass gap of the theory,  $\mu$ -terms can decay substantially slower with the volume in the case of weakly bound states. Moreover, even when they are expected to decay fast on the basis of the magnitude of their characteristic scale  $\mu$ , their contributions to matrix elements can still be enhanced. Measuring their contribution to energy levels is not enough to estimate the errors in matrix element and resonance width calculations.

It is important to stress that the ingredients essential to the observations made in this papers are not restricted to the two-dimensional setting. The description of particles as composites in subsection 3.2 is just the well-known quantum mechanical treatment of bound states as analytic continuation of scattering states to complex values of the momenta. In fact, the expression of  $\mu$ -term corrections to finite volume masses are not that much different in higher space-time dimensions [19], the only difference is the appearance of some (negative) powers of  $L$  (and numerical factors) in front of the exponential correction term. Concerning form factors, the matrix elements in quantum field theories of four (or indeed any) space-time dimensions share the essential feature with their two-dimensional counterparts that they have singularities corresponding to disconnected pieces and bound state poles<sup>2</sup>. Therefore they too can be expected to show rapid variation in kinematical domains close to these singularities. In fact, the difficult aspect of modeling the  $\mu$ -terms in higher dimensions is to have the necessary information about many-particle form factors, which is so readily provided by the bootstrap in integrable models.

### Acknowledgments

GT is grateful to B. Pozsgay and S. Katz for discussions. This work was partially supported by the Hungarian OTKA grants K75172 and K81461.

---

<sup>2</sup>The only special feature in two-dimensions is that so-called anomalous threshold singularities which are branch cuts in four dimensions, correspond to poles in two-dimensional theories [34].

# A Sine-Gordon breather form factors

## A.1 Spectrum and $S$ matrix

The fundamental excitations of the sine-Gordon model (2.1) are a doublet of soliton/antisoliton of mass  $M$ . Their exact  $S$  matrix can be written as [5]

$$\mathcal{S}_{i_1 i_2}^{j_1 j_2}(\theta, \xi) = S_{i_1 i_2}^{j_1 j_2}(\theta, \xi) S_0(\theta, \xi) \quad (\text{A.1})$$

where

$$\begin{aligned} S_{++}^{++}(\theta, \xi) &= S_{--}^{--}(\theta, \xi) = 1 \\ S_{+-}^{+-}(\theta, \xi) &= S_{-+}^{-+}(\theta, \xi) = S_T(\theta, \xi) \\ S_{+-}^{-+}(\theta, \xi) &= S_{-+}^{+-}(\theta, \xi) = S_R(\theta, \xi) \end{aligned}$$

and

$$\begin{aligned} S_T(\theta, \xi) &= \frac{\sinh\left(\frac{\theta}{\xi}\right)}{\sinh\left(\frac{i\pi-\theta}{\xi}\right)}, \quad S_R(\theta, \xi) = \frac{i \sin\left(\frac{\pi}{\xi}\right)}{\sinh\left(\frac{i\pi-\theta}{\xi}\right)} \\ S_0(\theta, \xi) &= -\exp\left\{-i \int_0^\infty \frac{dt}{t} \frac{\sinh\frac{\pi(1-\xi)t}{2}}{\sinh\frac{\pi\xi t}{2} \cosh\frac{\pi t}{2}} \sin\theta t\right\} \\ &= -\left(\prod_{k=1}^n \frac{ik\pi\xi - \theta}{ik\pi\xi + \theta}\right) \exp\left\{-i \int_0^\infty \frac{dt}{t} \sin\theta t\right. \\ &\quad \left.\times \frac{\left[2 \sinh\frac{\pi(1-\xi)t}{2} e^{-n\pi\xi t} + (e^{-n\pi\xi t} - 1)(e^{\pi(1-\xi)t/2} + e^{-\pi(1+\xi)t/2})\right]}{2 \sinh\frac{\pi\xi t}{2} \cosh\frac{\pi t}{2}}\right\} \end{aligned}$$

(the latter representation is valid for any value of  $n \in \mathbb{N}$  and makes the integral representation converge faster and further away from the real  $\theta$  axis).

Besides the solitons, the spectrum of theory contains also breathers  $B_r$ , with masses

$$m_r = 2M \sin \frac{r\pi\xi}{2} \quad (\text{A.2})$$

The breather-soliton and breather-breather  $S$ -matrices are also explicitly known [5].

## A.2 Breather form factors

We only consider exponentials of the bosonic field  $\Phi$ . To obtain matrix elements containing the first breather, one can analytically continue the elementary form factors of sinh-Gordon theory obtained in [35] to imaginary values of the couplings. The result is

$$\begin{aligned} \underbrace{F_{11\dots 1}^a}_n(\theta_1, \dots, \theta_n) &= \langle 0 | e^{ia\beta\Phi(0)} | B_1(\theta_1) \dots B_1(\theta_n) \rangle \\ &= \mathcal{G}_a(\beta) [a]_\xi (i\bar{\lambda}(\xi))^n \prod_{i<j} \frac{f_\xi(\theta_j - \theta_i)}{e^{\theta_i} + e^{\theta_j}} Q_a^{(n)}(e^{\theta_1}, \dots, e^{\theta_n}) \quad (\text{A.3}) \end{aligned}$$

where

$$\begin{aligned} Q_a^{(n)}(x_1, \dots, x_n) &= \det [a + i - j]_\xi \sigma_{2i-j}^{(n)}(x_1, \dots, x_n)_{i,j=1,\dots,n-1} \text{ if } n \geq 2 \\ Q_a^{(1)} &= 1, \quad [a]_\xi = \frac{\sin \pi\xi a}{\sin \pi\xi} \\ \bar{\lambda}(\xi) &= 2 \cos \frac{\pi\xi}{2} \sqrt{2 \sin \frac{\pi\xi}{2}} \exp\left(-\int_0^{\pi\xi} \frac{dt}{2\pi} \frac{t}{\sin t}\right) \end{aligned}$$

and

$$\begin{aligned}
f_\xi(\theta) &= v(i\pi + \theta, -1)v(i\pi + \theta, -\xi)v(i\pi + \theta, 1 + \xi) \\
&\quad v(-i\pi - \theta, -1)v(-i\pi - \theta, -\xi)v(-i\pi - \theta, 1 + \xi) \\
v(\theta, \zeta) &= \prod_{k=1}^N \left( \frac{\theta + i\pi(2k + \zeta)}{\theta + i\pi(2k - \zeta)} \right)^k \exp \left\{ \int_0^\infty \frac{dt}{t} \left( -\frac{\zeta}{4 \sinh \frac{t}{2}} - \frac{i\zeta\theta}{2\pi \cosh \frac{t}{2}} \right. \right. \\
&\quad \left. \left. + (N + 1 - Ne^{-2t}) e^{-2Nt + \frac{it\theta}{\pi}} \frac{\sinh \zeta t}{2 \sinh^2 t} \right) \right\} \tag{A.4}
\end{aligned}$$

gives the minimal  $B_1 B_1$  form factor<sup>3</sup>, while  $\sigma_k^{(n)}$  denotes the elementary symmetric polynomial of  $n$  variables and order  $k$  defined by

$$\prod_{i=1}^n (x + x_i) = \sum_{k=0}^n x^{n-k} \sigma_k^{(n)}(x_1, \dots, x_n)$$

Furthermore

$$\begin{aligned}
\mathcal{G}_a(\beta) = \langle e^{ia\beta\Phi} \rangle &= \left[ \frac{M\sqrt{\pi}\Gamma\left(\frac{4\pi}{8\pi-\beta^2}\right)}{2\Gamma\left(\frac{\beta^2/2}{8\pi-\beta^2}\right)} \right]^{\frac{a^2\beta^2}{4\pi}} \exp \left\{ \int_0^\infty \frac{dt}{t} \left[ -\frac{a^2\beta^2}{4\pi} e^{-2t} \right. \right. \\
&\quad \left. \left. + \frac{\sinh^2\left(\frac{a}{4\pi}t\right)}{2 \sinh\left(\frac{\beta^2}{8\pi}t\right) \cosh\left(\left(1 - \frac{\beta^2}{8\pi}\right)t\right) \sinh t} \right] \right\} \tag{A.5}
\end{aligned}$$

is the exact vacuum expectation value of the exponential field [36], with  $M$  denoting the soliton mass related to the coupling  $\lambda$  in (2.2) via [37]

$$\lambda = \frac{2\Gamma(\Delta)}{\pi\Gamma(1-\Delta)} \left( \frac{\sqrt{\pi}\Gamma\left(\frac{1}{2-2\Delta}\right) M}{2\Gamma\left(\frac{\Delta}{2-2\Delta}\right)} \right)^{2-2\Delta}, \quad \Delta = \frac{\beta^2}{8\pi} \tag{A.6}$$

Formula (A.3) also coincides with the result given in [38]. Form factors containing higher breathers can be obtained using that  $B_n$  is a bound state of  $B_1$  and  $B_{n-1}$ ; therefore sequentially fusing  $n$  adjacent first breathers gives  $B_n$ . Following the lines of reasoning of Appendix A of the paper [11] one obtains

$$\begin{aligned}
F_{k_1 \dots k_r n l_1 \dots l_s}^a(\theta_1, \dots, \theta_r, \theta, \theta'_1, \dots, \theta'_s) &= \tag{A.7} \\
\langle 0 | e^{ia\beta\Phi(0)} | B_{k_1}(\theta_1) \dots B_{k_r}(\theta_r) B_n(\theta) B_{l_1}(\theta'_1) \dots B_{l_s}(\theta'_s) \rangle &= \gamma_{11}^2 \gamma_{12}^3 \dots \gamma_{1n-1}^n \\
\times F_{k_1 \dots k_r \underbrace{l_1 \dots l_s}_n}^a \left( \theta_1, \dots, \theta_r, \theta + \frac{1-n}{2}i\pi\xi, \theta + \frac{3-n}{2}i\pi\xi, \dots, \theta + \frac{n-1}{2}i\pi\xi, \theta'_1, \dots, \theta'_s \right)
\end{aligned}$$

where

$$\gamma_{1k}^{k+1} = \sqrt{\frac{2 \tan \frac{k\pi\xi}{2} \tan \frac{(k+1)\pi\xi}{2}}{\tan \frac{\pi\xi}{2}}} \tag{A.8}$$

---

<sup>3</sup>The formula for the function  $v$  is in fact independent of  $N$ ; choosing  $N$  large extends the width of the strip where the integral converges and also speeds up convergence.

is the  $B_1 B_k \rightarrow B_{k+1}$  coupling, defined as the residue of the appropriate scattering amplitude:

$$\begin{aligned}
i \left( \gamma_{1k}^{k+1} \right)^2 &= \operatorname{Res}_{\theta = \frac{i\pi(k+1)\xi}{2}} S_{1k}(\theta) \\
S_{1k}(\theta) &= \frac{\sinh \theta + i \sin \frac{\pi(k+1)\xi}{2}}{\sinh \theta - i \sin \frac{\pi(k+1)\xi}{2}} \frac{\sinh \theta + i \sin \frac{\pi(k-1)\xi}{2}}{\sinh \theta - i \sin \frac{\pi(k-1)\xi}{2}}
\end{aligned} \tag{A.9}$$

## References

- [1] L. Maiani and M. Testa, “Final state interactions from Euclidean correlation functions,” *Phys. Lett.* **B245** (1990) 585–590.
- [2] L. Lellouch and M. Luscher, “Weak transition matrix elements from finite-volume correlation functions,” *Commun. Math. Phys.* **219** (2001) 31–44, [arXiv:hep-lat/0003023 \[hep-lat\]](#).
- [3] C. Lin, G. Martinelli, C. T. Sachrajda, and M. Testa, “ $K \rightarrow \pi\pi$  decays in a finite volume,” *Nucl. Phys.* **B619** (2001) 467–498, [arXiv:hep-lat/0104006 \[hep-lat\]](#).
- [4] M. Luscher, “Signatures of unstable particles in finite volume,” *Nucl. Phys.* **B364** (1991) 237–254.
- [5] A. B. Zamolodchikov and A. B. Zamolodchikov, “Factorized S-matrices in two dimensions as the exact solutions of certain relativistic quantum field models,” *Annals Phys.* **120** (1979) 253–291.
- [6] G. Mussardo, “Off critical statistical models: Factorized scattering theories and bootstrap program,” *Phys. Rept.* **218** (1992) 215–379.
- [7] M. Karowski and P. Weisz, “Exact Form-Factors in (1+1)-Dimensional Field Theoretic Models with Soliton Behavior,” *Nucl. Phys.* **B139** (1978) 455.
- [8] A. N. Kirillov and F. A. Smirnov, “A representation of the current algebra connected with the SU(2) invariant Thirring model,” *Phys. Lett.* **B198** (1987) 506–510.
- [9] F. A. Smirnov, “Form-factors in completely integrable models of quantum field theory,” *Adv. Ser. Math. Phys.* **14** (1992) 1–208.
- [10] V. P. Yurov and A. B. Zamolodchikov, “Truncated conformal space approach to scaling Lee-Yang model,” *Int. J. Mod. Phys.* **A5** (1990) 3221–3246.
- [11] B. Pozsgay and G. Takacs, “Characterization of resonances using finite size effects,” *Nucl. Phys.* **B748** (2006) 485–523, [arXiv:hep-th/0604022](#).
- [12] B. Pozsgay and G. Takacs, “Form factors in finite volume I: form factor bootstrap and truncated conformal space,” *Nucl. Phys.* **B788** (2008) 167–208, [arXiv:0706.1445](#).
- [13] B. Pozsgay and G. Takacs, “Form factors in finite volume II: disconnected terms and finite temperature correlators,” *Nucl. Phys.* **B788** (2008) 209–251, [arXiv:0706.3605](#).



- [14] B. Pozsgay, “Luscher’s mu-term and finite volume bootstrap principle for scattering states and form factors,” *Nucl. Phys.* **B802** (2008) 435–457, [arXiv:0803.4445 \[hep-th\]](#).
- [15] Z. Bajnok, L. Palla, G. Takacs, and F. Wagner, “The k-folded sine-Gordon model in finite volume,” *Nucl. Phys.* **B587** (2000) 585–618, [arXiv:hep-th/0004181](#).
- [16] G. Feher and G. Takacs, “Sine-Gordon form factors in finite volume,” *Nucl. Phys.* **B852** (2011) 441–467, [arXiv:1106.1901 \[hep-th\]](#).
- [17] M. Luscher, “Volume Dependence of the Energy Spectrum in Massive Quantum Field Theories. 2. Scattering States,” *Commun. Math. Phys.* **105** (1986) 153–188.
- [18] M. Luscher, “Two particle states on a torus and their relation to the scattering matrix,” *Nucl. Phys.* **B354** (1991) 531–578.
- [19] M. Luscher, “Volume Dependence of the Energy Spectrum in Massive Quantum Field Theories. 1. Stable Particle States,” *Commun. Math. Phys.* **104** (1986) 177.
- [20] T. R. Klassen and E. Melzer, “On the relation between scattering amplitudes and finite size mass corrections in QFT,” *Nucl. Phys.* **B362** (1991) 329–388.
- [21] G. Feverati, F. Ravanini, and G. Takacs, “Truncated conformal space at  $c = 1$ , nonlinear integral equation and quantization rules for multi-soliton states,” *Phys. Lett.* **B430** (1998) 264–273, [arXiv:hep-th/9803104](#).
- [22] G. Delfino, G. Mussardo, and P. Simonetti, “Non-integrable Quantum Field Theories as Perturbations of Certain Integrable Models,” *Nucl. Phys.* **B473** (1996) 469–508, [arXiv:hep-th/9603011](#).
- [23] G. Takacs, “Form factor perturbation theory from finite volume,” *Nucl. Phys.* **B825** (2010) 466–481, [arXiv:0907.2109](#).
- [24] G. Delfino and G. Mussardo, “Nonintegrable aspects of the multifrequency Sine-Gordon model,” *Nucl. Phys.* **B516** (1998) 675–703, [arXiv:hep-th/9709028 \[hep-th\]](#).
- [25] M. Fabrizio, A. O. Gogolin, and A. A. Nersisyan, “Critical properties of the double-frequency sine-Gordon model with applications,” *Nucl. Phys.* **B580** (2000) 647–687, [arXiv:cond-mat/0001227 \[cond-mat\]](#).
- [26] Z. Bajnok, L. Palla, G. Takacs, and F. Wagner, “Nonperturbative study of the two frequency sine-Gordon model,” *Nucl. Phys.* **B601** (2001) 503–538, [arXiv:hep-th/0008066](#).
- [27] G. Mussardo, V. Riva, and G. Sotkov, “Semiclassical particle spectrum of double Sine-Gordon model,” *Nucl. Phys.* **B687** (2004) 189–219, [arXiv:hep-th/0402179 \[hep-th\]](#).
- [28] G. Takacs and F. Wagner, “Double sine-Gordon model revisited,” *Nucl. Phys.* **B741** (2006) 353–367, [arXiv:hep-th/0512265](#).
- [29] J. Gasser and H. Leutwyler, “Light Quarks at Low Temperatures,” *Phys. Lett.* **B184** (1987) 83.

- [30] J. Gasser and H. Leutwyler, “Thermodynamics of Chiral Symmetry,” *Phys. Lett.* **B188** (1987) 477.
- [31] J. Gasser and H. Leutwyler, “Spontaneously Broken Symmetries: Effective Lagrangians at Finite Volume,” *Nucl. Phys.* **B307** (1988) 763.
- [32] S. R. Sharpe, “Quenched chiral logarithms,” *Phys. Rev.* **D46** (1992) 3146–3168, [arXiv:hep-lat/9205020](#) [hep-lat].
- [33] MILC Collaboration, C. Bernard, “Chiral logs in the presence of staggered flavor symmetry breaking,” *Phys. Rev.* **D65** (2002) 054031, [arXiv:hep-lat/0111051](#) [hep-lat].
- [34] S. R. Coleman and H. Thun, “On the prosaic origin of the double poles in the sine-Gordon S matrix,” *Commun. Math. Phys.* **61** (1978) 31.
- [35] A. Koubek and G. Mussardo, “On the operator content of the sinh-Gordon model,” *Phys. Lett.* **B311** (1993) 193–201, [arXiv:hep-th/9306044](#).
- [36] S. L. Lukyanov and A. B. Zamolodchikov, “Exact expectation values of local fields in quantum sine-Gordon model,” *Nucl. Phys.* **B493** (1997) 571–587, [arXiv:hep-th/9611238](#).
- [37] A. B. Zamolodchikov, “Mass scale in the sine-Gordon model and its reductions,” *Int. J. Mod. Phys.* **A10** (1995) 1125–1150.
- [38] S. L. Lukyanov, “Form factors of exponential fields in the sine-Gordon model,” *Mod. Phys. Lett.* **A12** (1997) 2543–2550, [arXiv:hep-th/9703190](#).